Journal of Fluids and Structures (2000) **14,** 957–970
doi:10.1006/jfls.2000.0305, available online at http://www.idealibrary.com on IDEAL®

AN ASSESSMENT OF HYDROELASTICITY FOR VERY LARGE HINGED VESSELS

C.-H. Lee and J. N. Newman

Department of Ocean Engineering, Massachusetts Institute of Technology
Cambridge, MA 02139, U.S.A.

(Received 1 February 1999, and in final form 20 April 2000)

A computational analysis is presented for the effects of waves on very large hinged vessels consisting of several modules, connected by simple hinges. Two generic types of modules are considered: rectangular barges similar to the Megafloat prototype and semi-submersibles similar to those proposed for mobile offshore bases. Most of the computations are for configurations with five modules, each of length 300 m. The results include vertical motions, structural deflections, and hinge shear forces in head and oblique waves. A range of structural stiffness parameters is considered, to permit a quantitative assessment of the importance of hydroelasticity.

1. INTRODUCTION

Most configurations proposed for mobile offshore bases (MOBs) and floating airports are large modular structures. A typical MOB configuration consists of five semi-subs, each 300 m long, with flexible connections used between the modules to relieve the wave-induced bending moments. One of the important hydrodynamic issues is the extent of the hydroelastic effects due to structural deflection of the modules. The importance of hydroelastic effects is obvious for large continuous structures; but, if flexible connectors are used between the modules, the structural deflection of each module is reduced and the importance of hydroelasticity is not so clear.

To address this issue we perform computations based on the assumptions of linearized inviscid wave motions. Only the vertical modes of motion are considered, and the structural deflections are governed by the beam equation. Two generic types of module are considered. The first is a rectangular "barge" with length 300 m, beam 80 m, and draft 6 m. The second is a semi-submersible of the same length and displacement, with rectangular pontoons and five circular columns above each pontoon. In both cases, the modules are joined by simple hinges with transverse axes. The barge shape was adopted initially to simplify the geometry, but it may be of direct interest since it is similar to the Megafloat floating airport.

The computational analysis is complicated by the geometrical complexity of the structures, large horizontal dimensions relative to the wavelength, and by the need to include a large number of modes of motion. To overcome these complications we use the higher-order panel code HIPAN, which represents the solution for the velocity potential by B-splines of arbitrary order. An earlier versions of this program is described by Lee *et al.* (1996). Two extensions have been made which facilitate the present analysis: (i) the body surface can be defined exactly, by an appropriate subroutine, instead of by B-spline approximations, as described by Lee (1997); and (ii) generalized modes are included to represent the hinge deflections and also the structural deflection of each module.

0889–9746/00/100957 + 14 $35.00/0

Following a brief outline of the theory and computational approach, illustrative results are presented for the barge and semi-sub configurations. The significance of hydroelasticity is related to a nondimensional stiffness parameter S which corresponds physically to the ratio between the internal structural force due to bending of the modules and the corresponding hydrostatic restoring force. A broad range of stiffness is considered, including the limits where the modules are completely flexible ($S = 0$) and rigid ($S = \infty$). The limit $S = 0$ is useful to confirm the validity of the numerical solution and the completeness of the generalized modes.

In the limit of zero stiffness one expects the vertical deflections of the structure to follow the local incident wave motion, both in amplitude and phase. Surprisingly, we find that this simple behavior does not occur in general, and in some cases the vertical motions are magnified substantially by dynamic effects. The principal exception is a floating flexible mat of zero draft, which precisely follows the incident-wave elevation, but even a relatively small draft can affect the vertical motions substantially.

2. OUTLINE OF ANALYSIS

A Cartesian coordinate system (x, y, z) is used with $z = 0$ the undisturbed free surface, x positive toward the "bow" of the array, and z positive upwards. The array is composed of N identical modules, each of which is symmetric about the vertical centerplane $y = 0$ and also about its midship section. The origin $x = 0$ is at the midpoint of the array. Simple transverse hinge joints are located at $x = x_n$ $(n = 1, 2, \dots, N-1)$, in the plane $z = 0$. The module ends are numbered in ascending order from the stern $(x = x_0)$ to the bow $(x = x_N)$. The overall length L of each module is defined as the distance between adjacent hinges, $x_{n+1} - x_n$. To simplify the analysis we neglect surge.

The vertical elevation at a position x along the array, due to the superposition of all vertical motions and bending deflections, is defined in the form $\mathrm{Re}\,(\xi(x)\,e^{i\omega t})$. This elevation is continuous along the array, and governed by the beam equation

$$-\omega^2 m\xi + (EI\xi'')'' = Z(x), \tag{1}$$

where m is the mass per unit length, E is the modulus of elasticity, and I denotes the moment of inertia for the cross-sectional area of the structure. Primes denote differentiation with respect to x, and $Z(x)$ is the local pressure force acting on a vertical section of unit length along the array.

The appropriate boundary conditions imposed on the structure are (i) the structural moment vanishes at the two ends and also at each hinge, (ii) the shear force vanishes at the two ends, and (iii) the shear force is continuous at each hinge.

The elevation ξ may be expanded in an appropriate set of modes, in the form

$$\xi(x) = \sum_j \xi_j f_j(x), \tag{2}$$

where ξ_j is the complex amplitude of each mode. If the modules are rigid, the appropriate modes will include heave and pitch of the entire array, moving as a rigid body, and $N-1$ hinge deflections defined by "tent" functions with unit amplitude at one hinge, decreasing linearly to zero at the adjacent hinges or ends of the array. The structural deflection of each module is represented by a set of Fourier sine modes, $\sin(k\pi u)$ $(k = 1, 2, 3, \dots)$, where $0 \le u \le 1$ is a normalized longitudinal coordinate defined separately on each module. In addition to these modes, which represent the actual physical motion of the array, $N-1$

discontinuous shear modes are used for computational convenience to evaluate the vertical shear forces acting on the hinges.

Adopting the method of weighted residuals and extending the analysis of Newman (1994) to account for the boundary conditions at the hinges, we obtain the linear system of equations

$$\sum_j \xi_j[-\omega^2(a_{ij}+M_{ij})+\mathrm{i}\omega b_{ij}+(c_{ij}+C_{ij})]=X_i. \tag{3}$$

Here a_{ij}, b_{ij}, and c_{ij} are the added-mass, damping, and hydrostatic restoring coefficients corresponding to the rigid-body and generalized modes, and X_i the exciting forces. The additional coefficients on the left-hand side are the mass and stiffness matrices

$$M_{ij}=\sum_{n=1}^{N}\int_{x_{n-1}}^{x_n} mf_i(x)f_j(x)\,\mathrm{d}x, \tag{4}$$

$$C_{ij}=\sum_{n=1}^{N}\int_{x_{n-1}}^{x_n} EIf_i''(x)f_j''(x)\,\mathrm{d}x. \tag{5}$$

In the examples to follow we assume that the mass per unit length m and stiffness EI are uniform along the length of each module. It is convenient to define the nondimensional stiffness parameter

$$S=EI/\rho gL^5, \tag{6}$$

which is used hereafter.

Since the structure is symmetrical about the planes $x=0$ and $y=0$, it is most efficient to redefine the modes in terms of their corresponding symmetric and antisymmetric components, with respect to x. Figure 1 shows the resultant sets of modes used for the computations with $N=5$ modules, to represent the hinge deflections and the first two ($k=1, 2$) sets of Fourier modes.

It should be emphasized in this approach that the entire structure is treated as a single 'global body' and the modes are all defined over this entire surface. An alternative would be to treat each module as a separate body, with its own modes of rigid-body motion and with similar Fourier bending modes. This alternative is somewhat simpler to interpret physically, but it has two significant disadvantages: (i) it is necessary to impose hard constraints in the equations of motion to represent the hinges, and (ii) it is not possible to exploit the longitudinal symmetry of the array.

3. ARRAY OF FIVE BARGES

Here we consider an array consisting of five rectangular barge modules, in head waves. Each module has a length $L=300$ m, beam $B=80$ m, and draft 6 m. One quadrant ($0<x<2{\cdot}5L, 0<y<B/2$) is represented by three patches on the bottom, three on the side, and one on the end, with separate patches on each module. Cubic B-splines are used to represent the velocity potential on each patch. The patches are subdivided into panels, with B-spline knots at the intersections of adjacent panels. For these computations each barge is subdivided longitudinally into 16 panels (eight on the forward half of the middle barge), vertically into two panels, transversely into two panels on half of the bottom and four panels across half of the end.

The maximum order of the Fourier bending modes on each module is $k=18$; there are a total of 96 modes of motion including heave, pitch, four hinge deflections, and 90 bending modes. The results are estimated to be accurate within the graphical precision of the figures, except possibly for some loss of accuracy for small values of S at wave periods below 10 s.

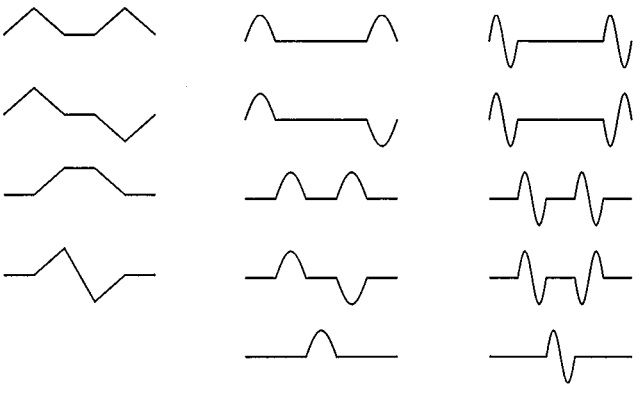

Figure 1. The hinge deflection modes and first and second ($k = 1, 2$) bending modes for the array with $N = 5$ modules, represented in terms of their symmetric and antisymmetric components.

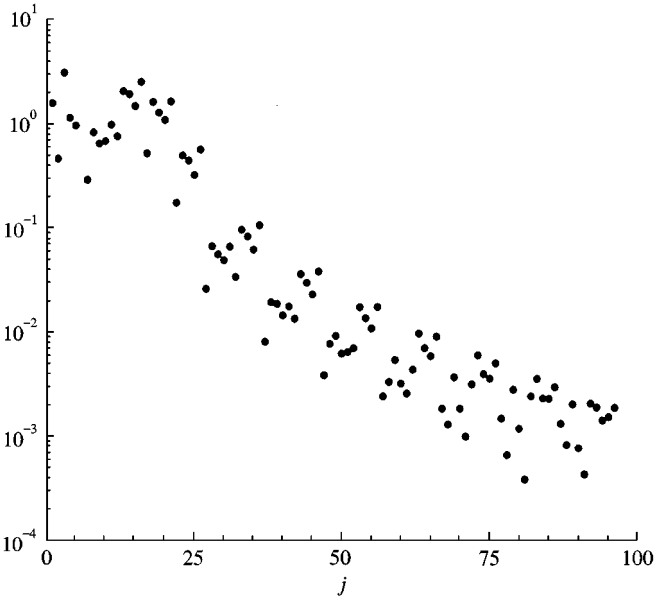

Figure 2. RAO in each mode j at period 12 s. The RAO for heave ($j = 1$) and all generalized mode RAOs ($j \geq 3$) are defined as $|\xi_j|/A$, where A is the incident-wave amplitude. The pitch RAO ($j = 2$) is multiplied by the half-length of the overall array to give the vertical motion amplitue at the bow or stern, per unit incident-wave amplitude.

Figure 2 shows the response amplitude (RAO) per unit incident-wave amplitude of each mode at the period of 12 s, for the case $S = 0$ where the modules are completely flexible. The modes with maximum response are $j = 3$, the first hinge mode, and $j = 13$ and 16 which correspond to the second and fifth modes in the third column of Figure 1. For larger values of j the RAOs decay in magnitude, confirming the convergence of the expansion (2).

Figure 3 shows the RAOs for the vertical motion at the bow, stern, and each hinge. The wave period ranges from 6 to 30 s, and values of the stiffness coefficient S are indicated in the legends of each figure. In long waves the RAOs are asymptotic to 1·0, as expected, and for short waves the RAOs tend to zero for the relatively stiff cases. For the rigid case there is a peak response at the bow of about 2·0 at a period of 19 s. As the stiffness is reduced the

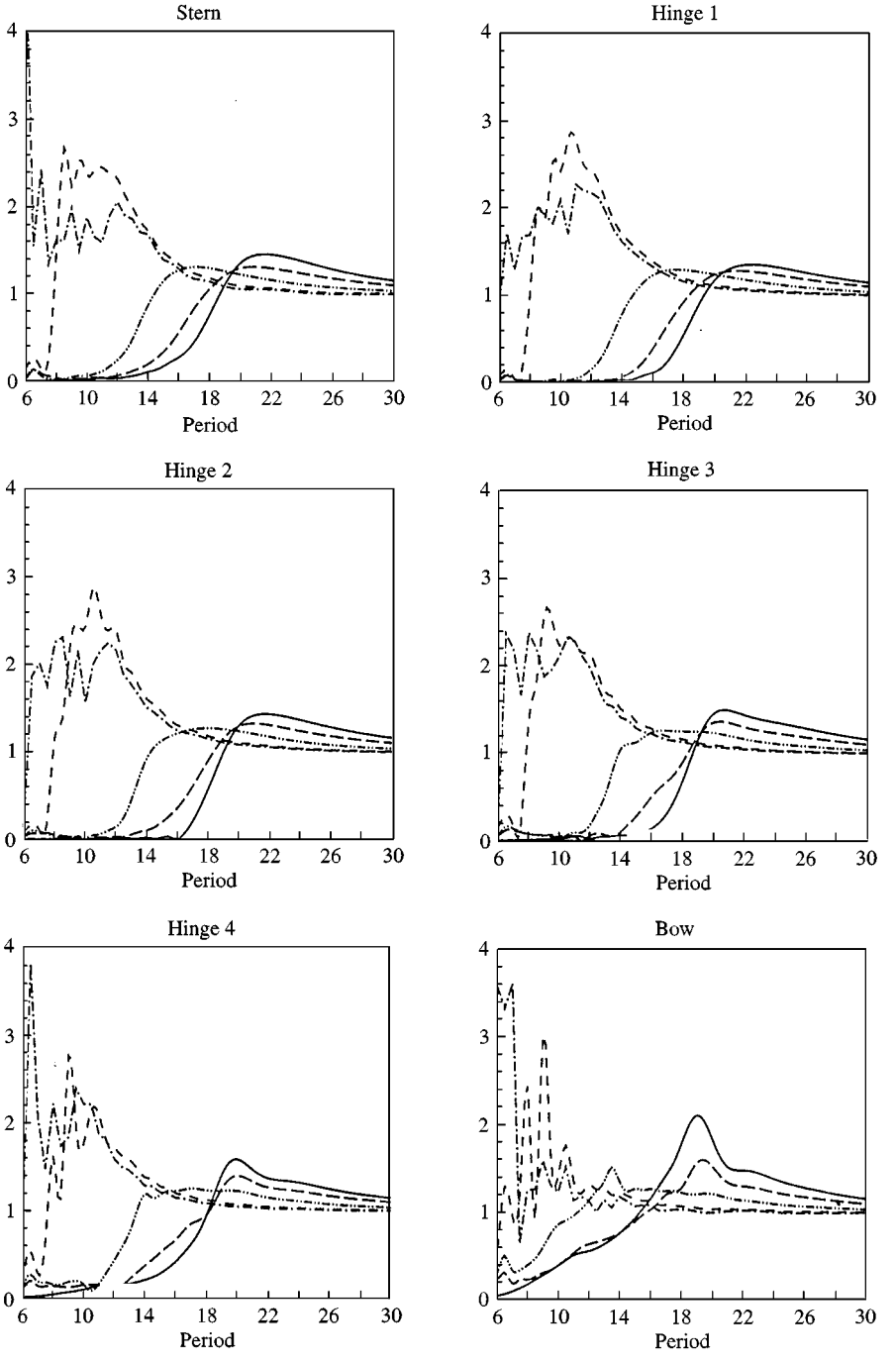

Figure 3. Amplitude of vertical motion per unit incident-wave amplitude (RAO) at the stern, hinges, and bow of the 5-module array of barges: ——, rigid; — — — —, $S = 10^{-3}$; —·—·—·—, $S = 10^{-4}$; - - - -, $S = 10^{-6}$; ·-·-·-·, $S = 0$. The nondimensional stiffness factor S is defined in equation (6).

peak response is shifted to lower periods, and the RAOs at the after hinges and stern are increased by the structural deflections of these modules.

Similar computations have been made for values of the stiffness coefficient $S = 0{\cdot}1$ and $0{\cdot}01$ but these are practically the same as for the rigid case. For $S = 10^{-8}$ the motions are practically the same as for zero stiffness. Thus, the range where hydroelastic effects have a significant effect on the motions is $10^{-6} < S < 10^{-3}$.

A surprising feature of these results is that the RAOs do not tend uniformly to 1.0 when $S \to 0$, as might be expected from the analogous results for a flexible floating mat of zero draft (Newman *et al.* 1996). This apparent paradox can be explained by estimating the relative importance of the added-mass and inertia coefficients, as functions of the mode index j. For moderate wave periods where the wavelength λ is comparable to or shorter than L, the maximum exciting force and response occur for the modes which have characteristic wavelengths similar to λ, including both the hinge modes and low-order Fourier modes, as confirmed in Figure 2. However, unlike the more familiar case of a heaving flat rigid body where the added mass dominates the body mass, the hydrodynamic coefficients for the relevant modes decrease rapidly with increasing mode index

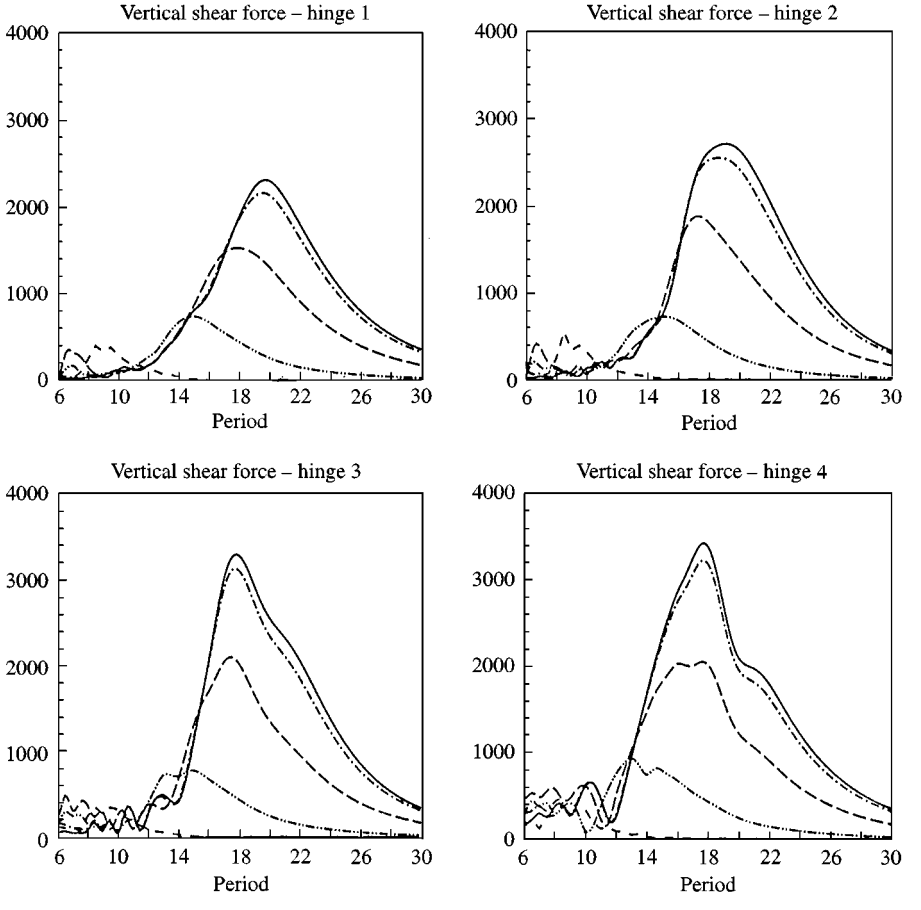

Figure 4. Vertical shear force acting on each hinge of the array with five barges: ——, rigid; —·—·—·—, $S = 10^{-2}$; — — — —, $S = 10^{-3}$; —··—··—··—, $S = 10^{-4}$; - - - -, $S = 10^{-6}$. The shear forces are normalized by the product $\rho g A \ell^2$, where ρ is the fluid density, g gravity, A the incident wave amplitude, and ℓ^2 is a reference area equal to 1 m^2.

j due to the longitudinal interference effect. Thus, the inertia coefficients (4), which do not decrease in the same manner, are comparable in importance to the added mass, and even a small draft (and proportional mass m) are significant. In the present case, the draft of 6 m is extremely shallow relative to the beam and length, but the corresponding displacement and body mass affect the motions substantially, as indicated by RAOs around 2·0 for the case $S = 0$ in wave periods up to 12 s (Fig. 4).

One of the most important issues in the design of hinged structures is the shear force which acts on the hinges. The plots in Figure 3 address this issue. The peak shear forces occur for this structure in the 18–20 s range of wave periods, with maximum values on the forward hinges. Decreasing the stiffness of the modules tends to reduce the shear forces, as expected. The case $S = 10^{-2}$ is practically the same as for rigid modules, whereas $S = 10^{-6}$ is nearly equivalent to zero stiffness. Thus, we conclude that the important regime for significant hydroelastic effects on the shear forces is $10^{-6} < S < 10^{-2}$.

More extensive results for a similar geometry have been developed by Newman (1998).

4. ARRAY OF SEMI-SUBS

Next, we consider an array of five hinged semi-subs, which will be referred to hereafter as a 'MOB'. Each semi-sub is 300 m long between hinges. The submerged part, shown in Figure 5, has a length of 260 m and draft 30 m. Each pontoon is 20 m wide with semi-circular ends; 40 m gaps separate the pontoons longitudinally and transversely. The columns are circular cylinders with radius 8 m, draft 20 m, and 60 m between the axes.

One quadrant of the MOB is represented by 42 patches and they are subdivided into 340 panels. Cubic B-splines are used to represent the velocity potential on each patch. The computational results are estimated to be accurate within 3% except near the resonance periods which will be discussed subsequently.

Although the geometry of the MOB is more complicated than the barge, we assume a uniform distribution of the mass and stiffness throughout the entire 300 m length in order to simplify the analysis. As in the previous section, heave, pitch, hinge modes and Fourier bending modes are used to represent the vertical dispacement. While the Fourier modes

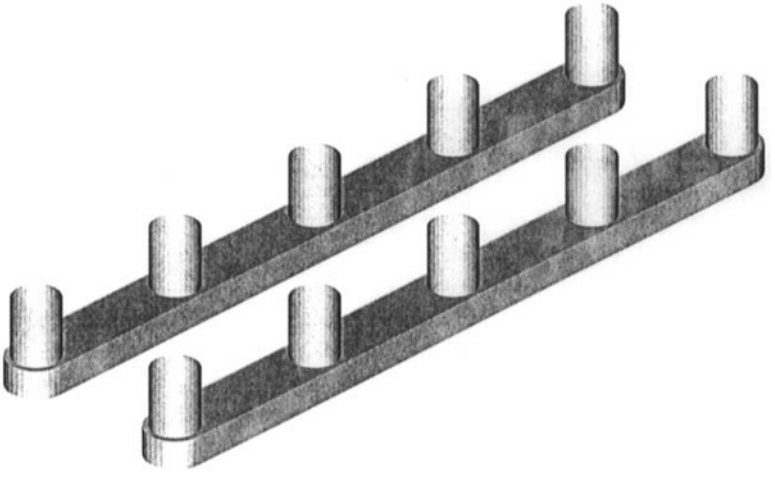

Figure 5. Submerged portion of one semi-sub.

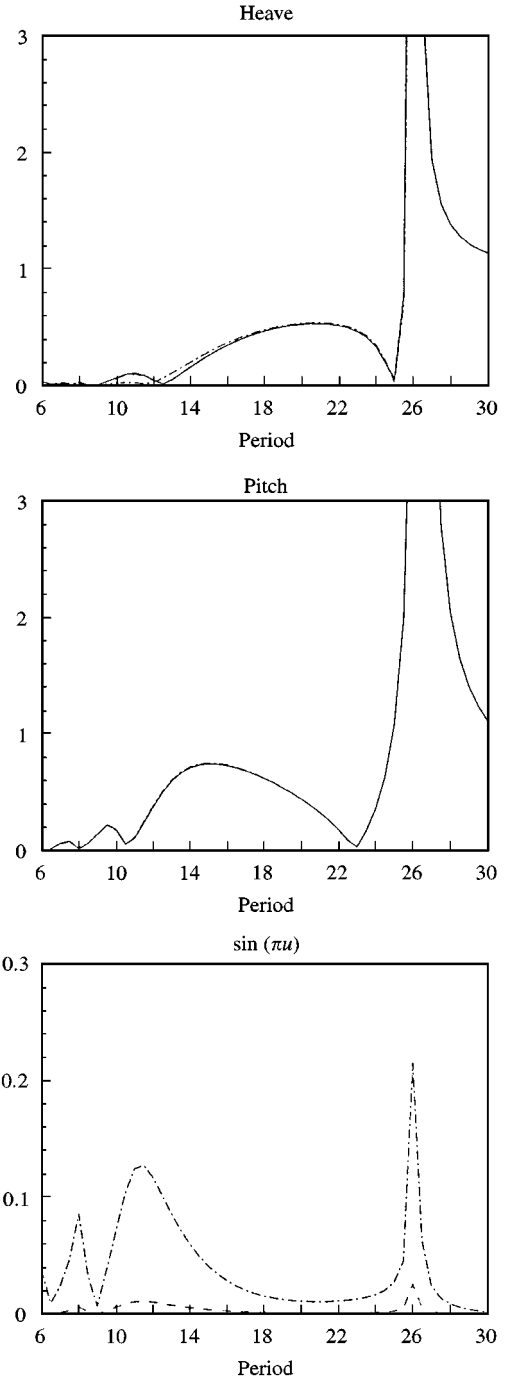

Figure 6. Response of a single module in head waves. For the heave and pitch modes: ———, rigid; — — — —, $S = 10^{-1}$; —·—·—·—, $S = 10^{-2}$; —··—··—··—, $S = 10^{-3}$. For the mode $\sin(\pi u)$: ———, $S = 10^{-1}$; - - - -, $S = 10^{-2}$; —·—·—·—, $S = 10^{-3}$. The normalization is as in Figure 2.

$\sin(k\pi u)$ are defined over the length of each module, $L = 300$ m, the hydrodynamic pressure acts over the length of the pontoon. The discontinuous loads at the ends of the pontoons (which drop to zero over the gaps) leads to, in principle, slow convergence of the Fourier modes expansion, unless the stiffness of the structure renders the higher mode responses insignificant. Thus, we limit our attention to a more practical range of the stiffness in this section.

We first consider a single isolated semi-sub. Figure 6 shows the RAOs for the heave, pitch and the first bending mode for head waves. Four different values of stiffness are considered, including a rigid module. The amplitudes of the higher bending modes are an order of magnitude smaller than the first bending mode and they are not included in the figure. The semi-sub experiences resonant heave motion near 26 s and the pitch resonance occurs at a slightly higher period. This highly tuned low-frequency resonance of the vertical modes is typical for the semi-sub because of its small water-plane area and small wave damping at low frequencies. In practice, however, the actual RAO may be reduced significantly due to viscous and nonlinear wave damping. Figure 6 also indicates values of the RAOs close to zero, at several periods where the wave exciting forces are small. At the period just below the resonance, where the scattering effects is relatively small, the Froude–Krylov exciting force vanishes because of the cancellation of the pressure forces between the top and bottom surface of the pontoon. The near-zero values for smaller periods occur at successive points where the product of wavenumber times length differ by about 2π, suggesting longitudinal interference effects similar to those predicted by slender-body theory.

As in the results in the previous section, the bending modes are insignificant for $S = 10^{-1}$ and $S = 10^{-2}$ and the results are practically the same as for the rigid module. For $S = 10^{-3}$ the structure experiences a significant bending. The large peak near 26 s is due to the coupling of the bending mode to the resonant heave mode. The large bending response over a broad range below 14 s is due to the natural bending modes.

Proceeding to the MOB configuration with five hinged modules, Figure 7 shows the RAOs for the vertical motion at the bow, stern and each hinge for head waves. For long waves the MOB experiences large heave and pitch resonance motions like a single rigid module. The symmetric elevation between fore and aft implies that the wave scattering is small for the semi-sub for the relatively long waves and the sheltering effect from the upwave modules is negligible. Thus, the RAO of the modules with free ends at the bow and stern is large and the RAO decreases towards the middle of the MOB. This differs from the case of the floating barges, where the elevation decreases in the downwave direction due to sheltering.

Figure 8 shows the hinge shear forces with the same normalization as in Figure 4. The large resonant heave and pitch motions for long waves do not induce significant shear force, since the relative motion between the modules is relatively small. For $S = 10^{-3}$, the shear force increases sharply below 14 s, in contrast to the floating barge where both the bending deflection and shear force are negligible. This is because the period of structural bending resonance increases when the structure is submerged, due to the increased added mass.

Figures 9 and 10 show the vertical elevations and shear forces induced by oblique waves at 45° incidence from the bow. Other than the increased wavelength along the longitudinal direction, the results are very similar to the head-wave case. This contrasts with computations for the barge array by Newman (1998) where the deflection and shear force are generally greater in oblique waves, except for the bow module. This difference between the two structures can be attributed to the stronger sheltering effect of the barge array in head waves and the absence of sheltering for oblique waves.

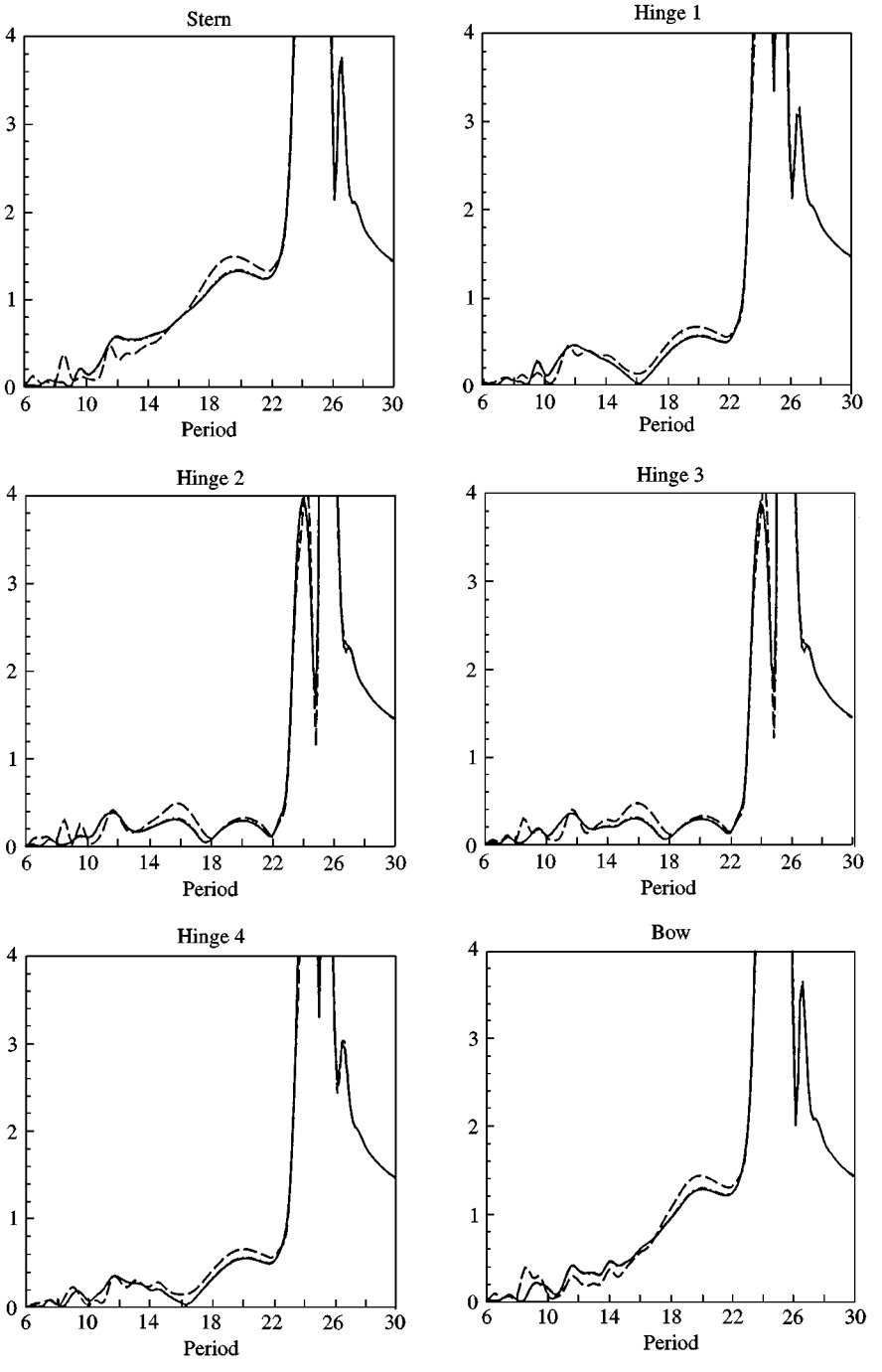

Figure 7. Amplitude of vertical motion per unit incident-wave amplitude (RAO) at the stern, hinges, and bow of the 5-module array of semi-subs in head waves: ———, rigid; - - - -, $S = 10^{-1}$; —·—·—·—, $S = 10^{-2}$; — — — —, $S = 10^{-3}$.

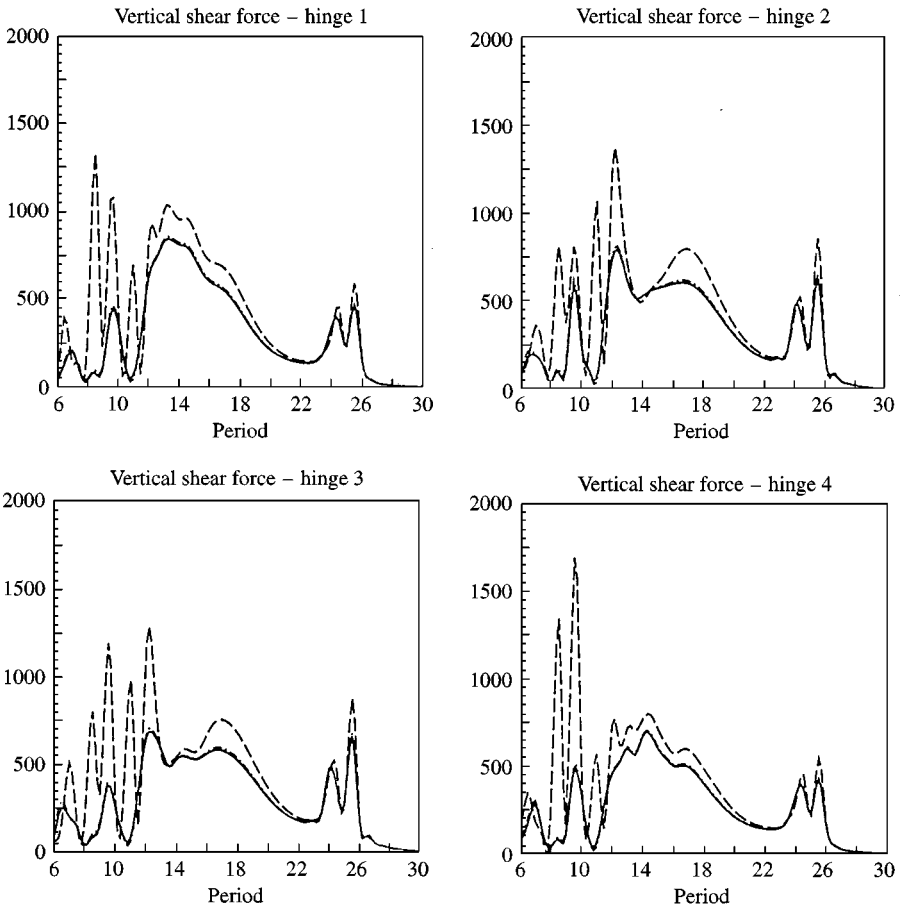

Figure 8. Vertical shear force acting on each hinge of the array with five semi-subs in head waves: ———, rigid; ----, $S = 10^{-1}$; —·—·—·—, $S = 10^{-2}$; — — — —, $S = 10^{-3}$.

5. CONCLUSIONS

A computational methodology has been developed to assess the effects of hydroelasticity on large arrays of hinged structures. The results demonstrate that it is feasible to analyze linearized wave interactions for several interacting semi-subs. The computations shown here are for generic structures and simple Fourier bending modes, but the same method can be used with more specific geometries and appropriate structural eigenmodes.

We have characterized the hydroelastic effects with the nondimensional stiffness parameter $S = EI/\rho g L^5$. Based on the length $L = 300$ m of each module we find that hydroelastic effects are important in the regime where, approximately, $10^{-6} < S < 10^{-2}$, and primarily within the narrower regime $10^{-4} < S < 10^{-3}$. For larger values of S the structure is effectively rigid, except for the hinge modes. For smaller values of S the structure effectively behaves like a completely flexible monohull. These estimates may vary somewhat depending on the specific geometry, and on the responses or loads considered, but we expect that their order of magnitude will be qualitatively similar in most practical applications.

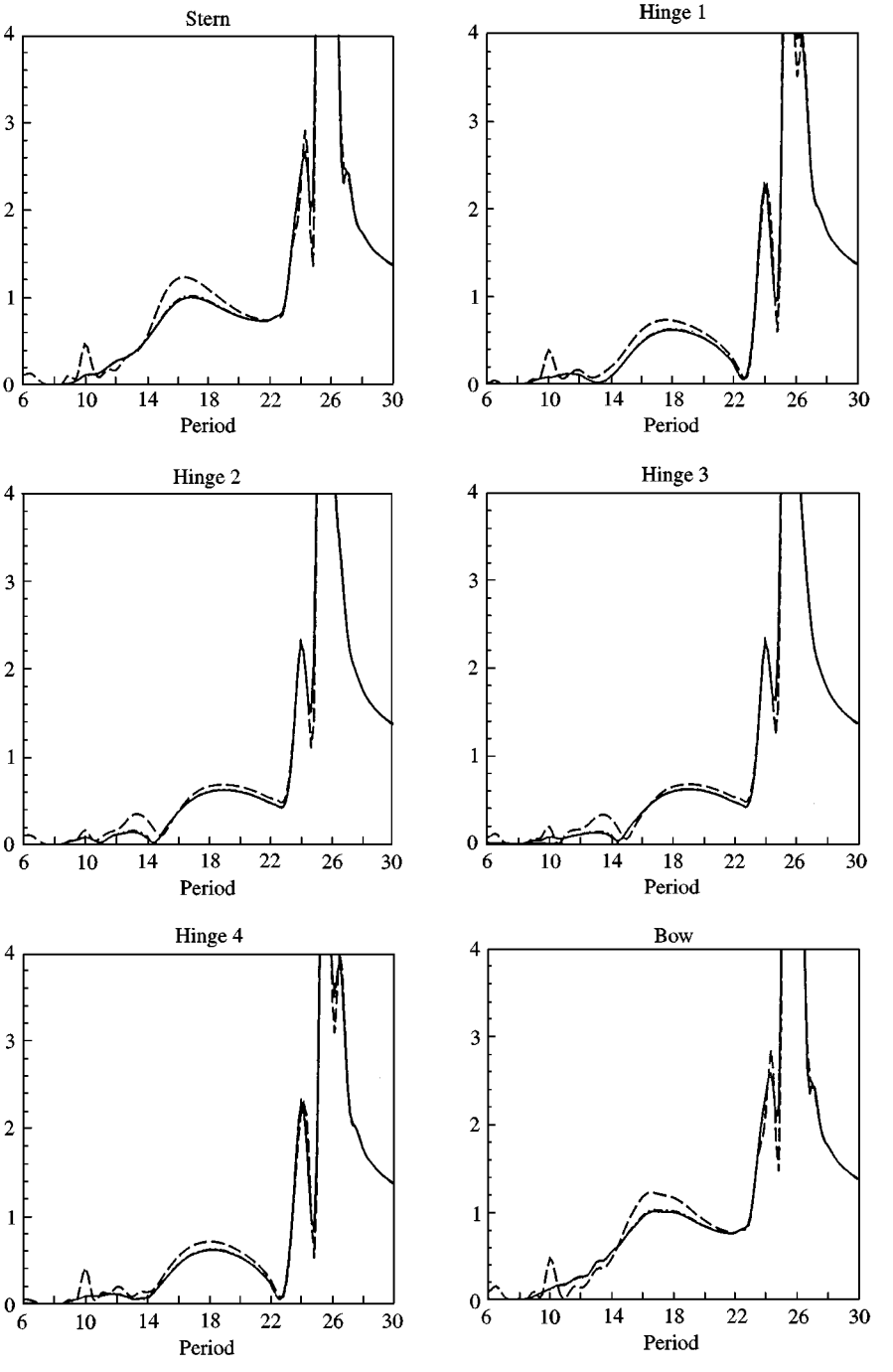

Figure 9. Amplitude of vertical motion per unit incident-wave amplitude (RAO) at the stern, hinges, and bow of the 5-module array of semi-subs at the 45° wave heading: ———, rigid; - - - -, $S = 10^{-1}$; —·—·—·—, $S = 10^{-2}$; — — — —, $S = 10^{-3}$.

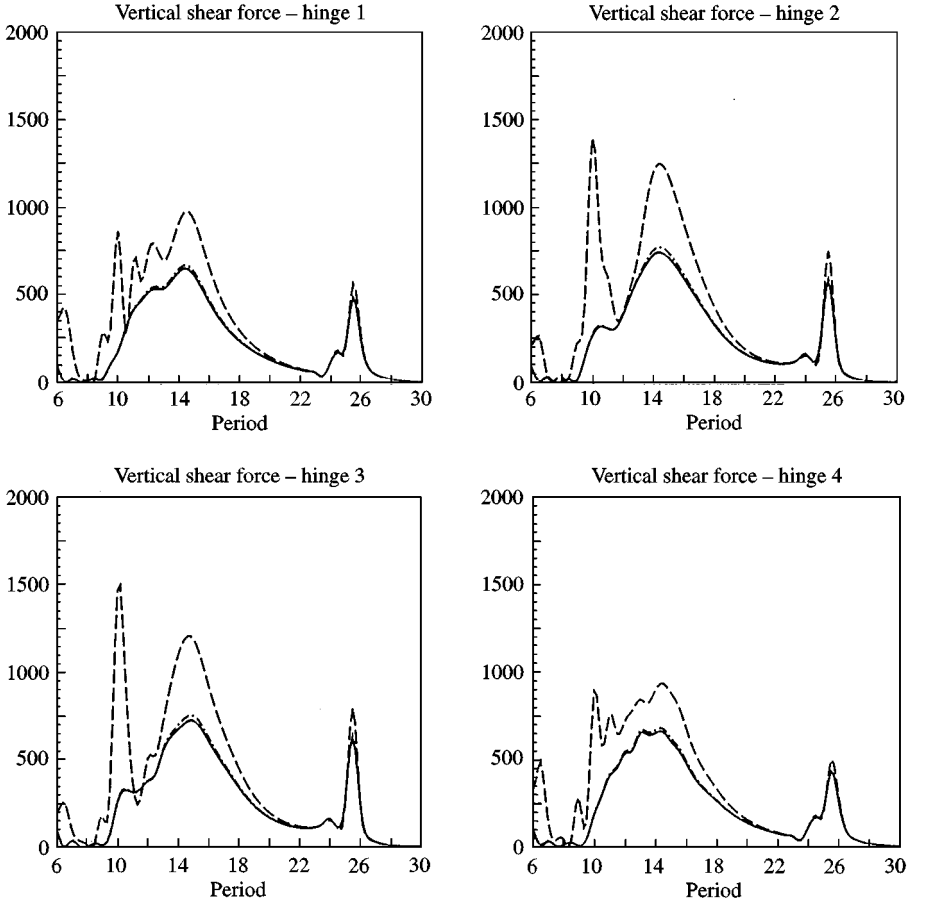

Figure 10. Vertical shear force acting on each hinge of the array with five semi-subs at the 45° wave heading: ———, rigid; - - - -, $S = 10^{-1}$; —·—·—·—, $S = 10^{-2}$; — — — —, $S = 10^{-3}$.

The limit $S = 0$ has been included in Section 3 to confirm that a sufficient number of bending modes are included to achieve convergence for a flexible structure, where the motion is progressive along the array in phase with the incident wave. However, the RAOs in this limit generally do not tend to the simple limit 1.0, as in the case of a flexible mat with zero draft. Even the relatively small draft of the barges considered here is significant in this context. Thus it is dangerous to idealize a large floating structure by a mat, unless the stiffness is sufficiently large to diminish the importance of the higher modes where the body inertia is significant.

Only the vertical motions and shear forces have been considered here. It is straightforward to extend the same methodology to include horizontal motions and loads. The consideration of torsional motion along the length is particularly important for the MOB configuration, and remains to be analyzed in future work.

These computations have been performed using the program HIPAN. The results in Section 3 were obtained on a 200 MHz PC, and those in Section 4 on a 433 MHz DEC Alpha workstation. The corresponding CPU times are on the order of 30 min per wave period, using a total of 100 modes for the barge and 55 modes for the MOB. In both cases,

we have exploited the capability of HIPAN to represent the geometry exactly. The MOB configuration based on five semi-subs is a complex structure from the geometric standpoint, even in the idealized form considered here. We have used a minimum number of patches, to define each semi-sub module in the form shown in Figure 5. A somewhat larger number of patches may be required to define a semi-sub where the shape is more irregular, with corresponding increases in the CPU time.

ACKNOWLEDGEMENTS

This work was supported by the Office of Naval Research, Grant N00014-97-1-0827, under the direction of the Naval Facilities Engineering Service Center. Additional support was provided by the Chevron Petroleum Technology Company, David Taylor Research Center, Exxon Production Research, Mobil Oil Company, Norsk Hydro, Offshore Technology Research Center, Petrobraś, Saga Petroleum, Shell Development Company, Statoil, and Det Norske Veritas.

References

Lee, C.-H. 1997 Wave interactions with huge floating structures. *Proceedings 8th International Conference on the Behaviour of Offshore Structures*, Vol. **2,** pp. 253–265, Delft, The Netherlands.

Lee, C.-H., Maniar, H., Newman, J. & Zhu, X. 1996 Computations of wave loads using a B-spline panel method. *Proceedings 21st Naval Hydrodynamics Symposium*, pp. 75–92, Trondheim, Norway.

Newman, J. N. 1994 Wave effects on deformable bodies. *Applied Ocean Research* **16,** 47–59.

Newman, J. N. 1998 Wave effects on hinged bodies; Part 4—vertical bending modes. *http//chf.mit.edu.*

Newman, J. N., Maniar, H. D. & Lee, C.-H. 1996 Analysis of wave effects for very large floating structures. *Proceedings International Workshop on Very Large Floating Structures VLFS '96*, pp. 34-1/8, Hayama, Japan.